Surface-enhanced Raman Scattering on Ordered Gold Nanodot Arrays Prepared from Anodic Porous Alumina Mask

Toshiaki Kondo,[1,2] Futoshi Matsumoto,[1] Kazuyuki Nishio,[1] and Hideki Masuda*[1]
[1]*Department of Applied Chemistry, Tokyo Metropolitan University, 1-1 Minamiosawa, Hachioji, Tokyo 192-0397*
[2]*Japan Society for the Promotion of Science, 1-1 Minamiosawa, Hachioji, Tokyo 192-0397*

(Received January 7, 2008; CL-080014; E-mail: masuda-hideki@c.metro-u.ac.jp)

We show surface-enhanced Raman scattering (SERS) on an ordered array of Au nanodots prepared from a highly ordered anodic porous alumina mask. The intensity of SERS signals is strongly dependent on the height of the Au dots, indicating the existence of optimum geometrical structures for SERS. The fabrication process of the nanodot array described in the present study enables easy preparation of SERS substrates.

The fabrication of functional devices based on the localized surface plasmon (LSP) in small metal particles has attracted increasing attention due to its application in various fields, such as chemical or biological sensing.[1–6] Precise control of the sizes and shapes of the small particles is important because the properties of LSP are substantially dependent on the geometrical structure of the metal particles.[7,8] In our previous work, we reported the fabrication of ordered nanodot arrays of metals on the substrate using anodic porous alumina masks and showed LSP properties of the obtained metal nanodot arrays.[9–12] In this process, metal nanodot arrays are prepared by vacuum deposition of metals through an anodic porous alumina mask with a highly ordered hole array structure. In the present work, we show, for the first time, SERS on the ordered array of Au nanodots prepared by vacuum deposition through a highly ordered anodic porous alumina mask. SERS on the metal fine structures is a typical phenomenon originating from the enhancement of the electric field of incident light. There have been numerous reports on the preparation of an ordered nanostructure of metals for optimizing the efficiency of SERS.[13,14] However, processes for easy precise control of the structure of metal particles have not been established. The advantage of the use of vacuum deposition using an anodic porous alumina mask for the preparation of the metal nanostructure for SERS is the controllability of the dimension of the dots in addition to the ease of preparation. Here, we describe the dependence of the SERS efficiency of pyridine on the geometrical structures of Au nanodot arrays on a Si substrate.

The procedure for the preparation of Au dot arrays is almost the same as reported previously.[8] Briefly, the anodic porous alumina used for the mask was prepared by the anodization of Al (99.99% purity) in acidic solution after the electrochemical polishing of Al. Porous alumina masks with through holes were obtained by the selective dissolution of Al in saturated I_2 methanol solution followed by the dissolution of the bottom part of the porous alumina films in phosphoric acid solution. The hole sizes of the alumina mask were adjusted by postetching treatment in phosphoric acid solution.

Au was vacuum deposited onto a Si substrate using a vacuum evaporator through the alumina mask, which was set up on the substrate. The thickness of the alumina mask was typically 240 nm. After the vacuum deposition, the Au nanodot array on the substrate was obtained by removing the alumina mask mechanically.

Raman scattering spectra of pyridine were obtained using a Raman scattering spectrometer equipped with a He-Ne laser (633 nm) as a light source. The size of laser spot was 13 μm. The laser power was 1.6 μW. The duration of irradiation and accumulation of signals were 3 s and 10 times, respectively. The Si substrate with the Au dot array was dipped in pyridine solution (HPLC grade, >99.9%) and dried in air before the measurement.

Figure 1 shows the SEM images of the typical Au nanodot array formed on the Si substrate. From the surface view in Figure 1a, it can be confirmed that uniformly sized dots are in an ordered arrangement with regular intervals. The size and interval of the Au dots were 70 and 100 nm, respectively. These values corresponded to the geometrical structure of the

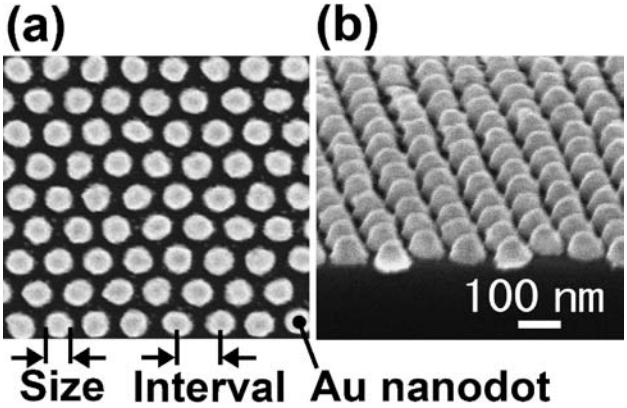

Figure 1. SEM image of Au dot array prepared using porous alumina mask; surface view (a) and oblique view (b).

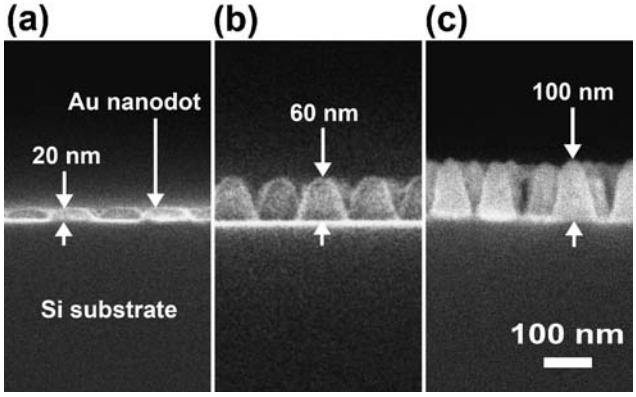

Figure 2. Cross-sectional SEM views of Au dot array; dot height of 20 (a), 60 (b), and 100 nm (c).

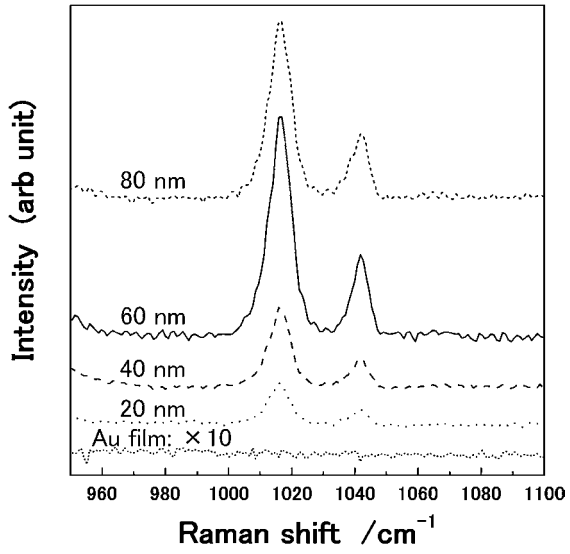

Figure 3. SERS spectra from Au dots array with different dot heights.

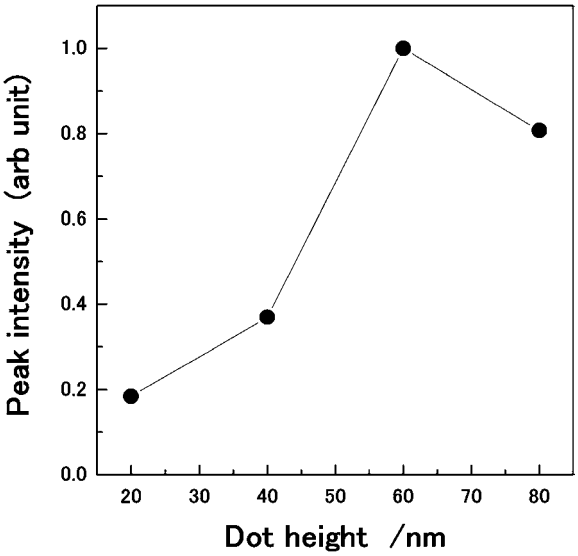

Figure 4. Dependence of SERS intensity on Au dot height.

porous alumina mask used for evaporation. The oblique view in Figure 1b shows the shape of the Au dots. The height of Au dots was 40 nm. The conical shape of the Au dots results from the shadowing effect of the mask during the vacuum deposition of Au.

In the present study, the effect of the height of Au dots on SERS was examined. Figure 2 shows SEM images indicating the variation of the height of the Au dots. The height of Au nanodots was controlled by changing the nominal thickness of the evaporated Au using a thickness monitor during the vacuum evaporation. The cross-sectional SEM images in Figure 2 revealed that the height of the Au dots was controlled from 20 to 100 nm. These heights corresponded to the aspect ratio (the height divided by the bottom size of dots) from 0.3 to 1.4.

Figure 3 shows the SERS spectra obtained from Au dot arrays with different dot heights. The deviation of peak intensity in the measurement was 20% for the same substrate. Compared to the spectrum from the smooth Au surface, the intensity of Raman scattering was confirmed to be enhanced on the Au dot arrays; that is, two characteristic peaks from the adsorbed pyridine molecules were observed at 1014 and 1040 cm^{-1}. The assignment of a slight peak observed at around 940 cm^{-1} could not be achieved at the present stage. Interestingly, the intensity of SERS is strongly dependent on the height of Au dots.

Figure 4 summarizes the dependence of SERS intensity on the height of Au dots. In Figure 4, the Raman intensities at 1014 cm^{-1} was summarized against the dot heights. The intensities were normalized by setting the value at the dot height of 60 nm to unity. The Raman intensity increased with the height of the Au dots and showed the highest value at the dot height of 60 nm. Although the detailed mechanism of the dependence of the SERS intensity on the height of Au dots is not clear at the present stage, one possible explanation is that the efficiency of absorption by LSP depends on the shape of dots and yields the change of SERS intensity. Such dependence of the efficiency of absorption by LSP on the shape of Au dots could be also supported by the three-dimensional FDTD simulation. The result in Figure 3 indicates that the optimal geometrical structures yield the highest efficiency of SERS. For such optimization of SERS efficiency, the process described in the present study will be useful because of its ease and controllability in the preparation of ordered Au nanodot arrays.

The SERS intensity from ordered Au nanodot arrays prepared using an anodic porous alumina mask was examined. The intensity was strongly dependent on the height of the Au dots, indicating the existence of optimum geometrical structures for SERS. The process described in the present study allows preparation of nanodot arrays of other metals on various kinds of substrates. The present process allows the easier preparation of SERS substrates compared to the process employing the electron beam lithographic technique. In addition, the geometrical structures of dots can be tuned to optimize the enhancement of SERS intensity. The obtained SERS substrates will be used for the Raman spectra measurement with high sensitivity.

This work was partially supported by Grant-in-Aid for Scientific Research No. 19049013 on Priority Area “Strong Photons–Molecules Coupling Fields (470)” from the Ministry of Education, Culture, Sports, Science and Technology of Japan.

References

1 K. Ueno, S. Juodkazis, M. Mino, V. Mizeikis, H. Misawa, *J. Phys. Chem. C* **2007**, *111*, 4180.
2 Y. Niidome, H. Takahashi, S. Urakawa, K. Nishioka, S. Yamada, *Chem. Lett.* **2004**, *33*, 454.
3 V. Malyarchuk, M. E. Stewart, R. G. Nuzzo, J. A. Rogers, *Appl. Phys. Lett.* **2007**, *90*, 203113.
4 N. Yang, X. Su, V. Tjong, W. Knoll, *Biosens. Bioelectron.* **2007**, *22*, 2700.
5 B. I. Ipe, K. Yoosaf, K. G. Thomas, *J. Am. Chem. Soc.* **2006**, *128*, 1907.
6 G. Duan, W. Cai, Y. Luo, Z. Li, Y. Li, *Appl. Phys. Lett.* **2006**, *89*, 211905.
7 C. L. Nehl, H. Liao, J. H. Hafner, *Nano Lett.* **2006**, *6*, 683.
8 F. Wang, Y. R. Shen, *Phys. Rev. Lett.* **2006**, *97*, 206806.
9 H. Masuda, M. Satoh, *Jpn. J. Appl. Phys.* **1996**, *35*, L126.
10 H. Masuda, K. Yasui, K. Nishio, *Adv. Mater.* **2000**, *12*, 1031.
11 F. Matsumoto, M. Ishikawa, K. Nishio, H. Masuda, *Chem. Lett.* **2005**, *34*, 508.
12 K. Yasui, Y. Sakamoto, K. Nishio, H. Masuda, *Chem. Lett.* **2005**, *34*, 342.
13 Y. Sawai, B. Takimoto, H. Nabika, K. Ajito, K. Murakoshi, *J. Am. Chem. Soc.* **2007**, *129*, 1658.
14 N. Félidj, J. Aubard, G. Lévi, J. R. Krenn, M. Salerno, G. Schider, B. Lamprecht, A. Leitner, F. R. Aussenegg, *Phys. Rev. B* **2002**, *65*, 075419.

Published on the web (Advance View) March 25, 2008; doi:10.1246/cl.2008.466